European Polymer Journal 239 (2025) 114305

Contents lists available at ScienceDirect

European Polymer Journal

journal homepage: www.elsevier.com/locate/europolj

Reactivity ratios of bio-based itaconates and acrylates in radical copolymerizations

Lennart Arendes [a,*], Marco Drache [a], Celine Bösche [b], Tobias Robert [b], Sabine Beuermann [a,*]

[a] Institute of Technical Chemistry, Clausthal University of Technology, Arnold-Sommerfeld-Strasse 4, 38678 Clausthal-Zellerfeld, Germany
[b] Fraunhofer Institute for Wood Research – Wilhelm-Klauditz-Institut WKI, Riedenkamp 3, 38108 Braunschweig, Germany

ARTICLE INFO

Keywords:
Itaconic acid esters
Acrylates
Bio-based monomer
Free-radical copolymerization
Reactivity ratio
Benchtop NMR spectrometer

ABSTRACT

Replacing petrochemically-based monomers by bio-based building blocks is an important topic in polymer chemistry. Recently, itaconic acid and its derivatives are investigated as potential alternatives. Free-radical polymerizations of these monomers are associated with a very low propagation rate. Moreover, the propagation reaction becomes reversible already at temperatures of 60 °C, which limits the accessible monomer conversion. To overcome these issues, copolymerizations with acrylates are attractive due to not being prone to depropagation at typical polymerization temperatures and fast propagation rates. Due to the presence of acrylate units in the copolymer higher monomer conversions are accessible compared to homopolymerizations. Since copolymer properties are strongly depending on the copolymer composition, their prediction via reactivity ratios (*r* values) is important. Here, *r* values determined via Monte Carlo simulations with consideration of depropagation are reported for several copolymerizations of three itaconates and four acrylates with non-functional ester groups. Polymer characterization is based on SEC elution curves and ^{1}H NMR spectra recorded with an 80 MHz benchtop NMR spectrometer. A common pair of reactivity ratios is obtained, with 1.50 and 0.54 for the itaconate and acrylate comonomer, respectively. It is shown that these *r* values can be transferred to other non-functional comonomer pairs.

1. Introduction

The increasing demand for sustainable and environmentally friendly polymeric materials has driven research towards the implementation of bio-based monomers as a replacement for petrochemical building blocks. In this respect, itaconic acid (IA) has emerged as a promising candidate, as it is already produced on an industrial scale at competitive cost via a biotechnological process.[1,2] In addition, IA was highlighted as one of the most important platform chemicals for green chemistry by the US Department of Energy in 2004. Due to its trifunctional nature, IA is a versatile building block that can be utilized in different types of polymerization reactions. The two carboxylic acid groups allow for its application in polycondensation reactions to synthesize (unsaturated) polyesters.[3] In addition, these carboxylic acid groups can be used to prepare a range of mono and diesters.[4–7] Finally, the conjugated double bond allows for the use of IA and its esters in radical polymerization reaction as an alternative to petrochemical (meth)acrylates.[8]

While free radical polymerizations (FRP) are particularly attractive for industrial applications due to their robustness and tolerance to impurities, FRP of itaconic acid and its derivatives are associated with low propagation rate coefficients, k_p, below 10 L•mol^{-1}•s^{-1} at 25 °C.[9–12] Moreover, the propagation reaction becomes reversible already at temperatures as low as 60 °C.[9,11] The effective propagation rate coefficient $k_{p,eff}$ is given by Eq. (1).[13]

$$k_{p,eff} = k_p - k_{dep}/c_M \quad (1)$$

k_{dep} refers to the depropagation rate coefficient and c_M to the monomer concentration. The equilibrium of propagation and depropagation depicted in Scheme 1 limits the accessible monomer conversion. At the equilibrium monomer concentration c_M^{eq} the effective propagation rate coefficient is zero. According to Eq. (1) c_M^{eq} is given by the ratio of k_{dep} and k_p.

To overcome these challenges copolymerizations of itaconates with significantly more reactive monomers such as (meth)acrylates are interesting. k_p of these monomers are several orders of magnitude higher than for the itaconates.[14,15] While depropagation of methacrylates has to be accounted for at temperatures roughly above 120 °C,[13]

* Corresponding author.
E-mail address: sabine.beuermann@tu-clausthal.de (S. Beuermann).

https://doi.org/10.1016/j.eurpolymj.2025.114305
Received 11 July 2025; Received in revised form 16 September 2025; Accepted 17 September 2025
Available online 20 September 2025

acrylates depropagate at much higher temperatures.[15] Thus, the presence of acrylates overcomes limited monomer conversion due to depropagation and favors higher polymerization rates.[16,17] To date, acrylates have not been produced entirely from renewable raw materials on an industrial scale. Nevertheless, there are partially bio-based acrylates such as isobornyl acrylate (iBoA) and 2-octyl acrylate (2OA), which contain 77 and 73 % bio-content, respectively.[18] These monomers contribute to a high bio-content in itaconate – acrylate copolymers. Another approach for enhancement of the polymerization rate is to apply emulsion polymerizations. Due to separation of macroradicals in different latex particles the probability of termination events is lowered compared to homogenous phase polymerizations.[19,20] It was already shown that emulsion polymerizations yield polymer with significant molar masses in acceptable reaction times.[21–23].

In order to tailor the copolymer composition and properties, the knowledge of the reactivity ratios is required. Mostly, reactivity ratios are determined based on the Lewis-Mayo equation with composition data from copolymerizations carried out up to low conversion. If the change of both monomer concentrations as a function of time is accessible, copolymerizations may be carried out over an extended conversion range. This approach is advantageous since a rather low number of experiments provides copolymer composition data over an extended range of monomer ratios.[24] This point is particularly attractive, e.g., for copolymerizations under unusual reaction conditions.[25] In particular in-line and off-line NMR spectroscopy was applied to monitor individual monomer conversions throughout copolymerizations.[26] Further, the amount of chemicals required is lower compared to performing a high number of low conversion reactions. Details on the evaluation of reactivity ratios were reported in a recent publication by an IUPAC Polymer Division working group.[24] The special case of copolymerizations with one of two monomers undergoing depropagation was addressed in a recent publication by Lundberg et al.[27].

Previously, it was shown that copolymerizations of butyl acrylate with either dibutyl itaconate (DBI) or dicyclohexyl itaconate (DCHI) yield copolymers with very similar compositions. Applying Monte Carlo simulation methods reactivity ratios of $r_{DBI/DCHI} = 1.26$ and $r_{BA} = 0.50$ were obtained, indicating that the itaconates are preferentially incorporated into the copolymer.[17] The finding is in agreement with a recent study on DBI-BA copolymerizations.[16] In order to identify the impact of the ester group on the copolymerization the study was extended to cyclohexyl acrylate (CHA), iBoA, and 2OA. Besides being synthesized from bio-based alcohols, iBoA and 2OA were selected, because (1) the isobornyl group is sterically demanding and leads to a high glass transition temperature T_G of 105 °C for poly(isobornyl acrylate),[28] and (2) the ester group of 2OA is very similar to 2-ethylhexyl acrylate, which is of high technical importance. CHA was chosen because the ester group is flexible and similar in size to BA. In addition, dimethyl itaconate (DMI) was selected, which allows for addressing the impact of a small itaconate ester group. All monomer structures are given in Fig. 1. The impact of ester groups largely varying in size and sterical demand were performed, since it was shown that the impact of the size of ester group on itaconate k_p is opposite to that generally observed for acrylates and methacrylates: while itaconate k_p decreases with increasing sterical demand of the ester group,[11] generally, k_p values of acrylates and methacrylates are increasing with ester size.[29] Moreover, for DMI, DBI, and DCHI the depropagation kinetics are known, which is important for the determination of reactivity ratios at 80 °C, where itaconate depropagation is already operative.[11] While in copolymerizations without depropagation the copolymer composition depends only on the comonomer ratio, in the case of depropagation the actual monomer concentration of the itaconate must also be taken into account. Therefore, established methods for determining the r values cannot be applied.

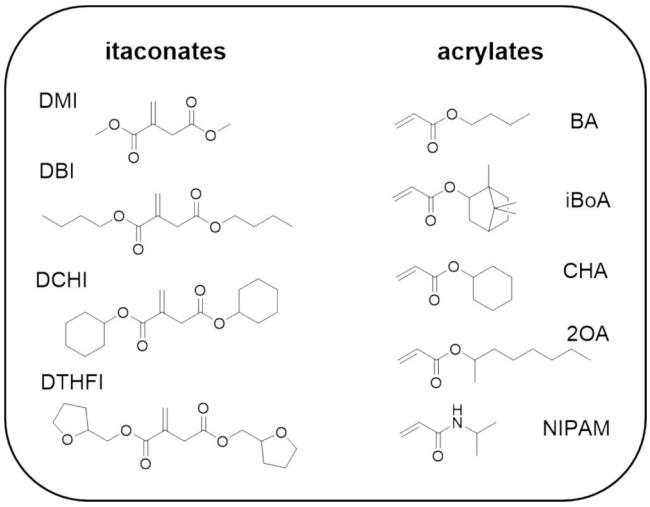

Fig. 1. Structures of the itaconate and acrylic monomers used in this study.

For ten comonomer systems with varying initial itaconate monomer feed compositions the derivation of r values is reported based on individual monomer concentrations determined as a function of reaction time from SEC analyses and ^{1}H NMR spectroscopy. The transferability of the r values is studied for two test comonomer systems with non-functional monomers.

2. Materials and methods

2.1. Materials

The monomers dibutyl itaconate (DBI, > 97.0 %, TCI), dimethyl itaconate (DMI, ≥ 98 %, TCI), butyl acrylate (BA, ≥99 %, Acros Organics), *i*-bornyl acrylate (iBoA, ≥ 90 %, TCI), cyclohexyl acrylate (CHA, ≥ 98 %, TCI), 2-octyl acrylate (2OA, ≥ 98 %, BASF), and N-isopropyl acrylamide (NIPAM, 98 %, TCI) were used without further purification. Dicyclohexyl itaconate (DCHI) was synthesized as detailed elsewhere.[4] 400 MHz NMR spectra were recorded in 1,4-*d*ioxane-d_8, (99 %, Deutero GmbH), 600 MHz NMR spectra were recorded in chloroform-d_1 (99.8 %, Deutero GmbH). Dioxane (99 %, Grüssing GmbH), THF (99.5 %, Roth), methanol (98.5 %, Walter CMP), hydroquinone (Riedel-de Haën, 99.5 %), 2,2′-azobis(isobutyronitrile) (AIBN, ≥ 98 %, Sigma-Aldrich), tetrahydrofuryl alcohol (98 %, TCI), itaconic acid (99 %, Merck), 4-methoxyphenol (99 %, Merck), and 3,5-di-*tert*-butyl-4-

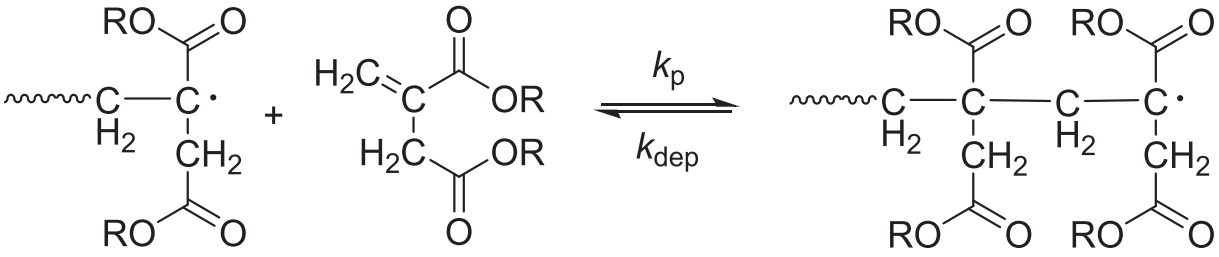

Scheme 1. Equilibrium of propagation and depropagation in itaconate polymerizations.

hydroxytoluene (99 %, Merck) were used as received. FASCAT® 4101 was kindly provided by PMC Group Inc. Dioxane was stored over KOH pellets.

2.2. Synthesis of ditetrahydrofurfuryl itaconate (DTHFI)

Itaconic acid (104.08 g, 0.8 mol) and tetrahydrofurfuryl alcohol (179.75 g, 1.76 mol) were placed into a 500 mL 3-neck round bottom flask equipped with a Dean-Stark apparatus and magnetic stirrer. Then 50 mg (0.02 wt%) 4-methoxyphenol, 70 mg (0.03 wt%) 3,5-di-*tert*-butyl-4-hydroxytoluene and 480 mg (0.20 wt%) FASCAT4101 were added. Subsequently 20 mL of toluene as an azeotropic solvent was added and the reaction mixture was step-wise heated to 170 °C. The reaction progress was monitored by the amount of water being collected in the Dean-Stark apparatus and the disappearance of the O–H-vibration of the carboxylic acid group in the infrared (IR). The toluene was then removed under reduced pressure and the crude product was dissolved in 1 L of ethyl acetate and extracted two times with 400 mL 2 M aqueous Na_2CO_3 solution. After removal of the ethyl acetate at reduced pressure, 222.1 g (93 % yield) of the DTHFI was obtained as yellow oil. NMR, IR and GC/MS spectra can be found in Fig. S1 to Fig. S3 of the supporting information.

2.3. Copolymerization procedure

The copolymerizations of an itaconate with an acrylate were carried out in solution with 50 vol% dioxane. Reaction mixtures of 6 and 14 mL were prepared for subsequent analysis by NMR and SEC, respectively. The monomer feed compositions are listed in Table S1 of the Supporting Information. Prior to polymerization the reaction mixture was purged with nitrogen for ten minutes to remove oxygen. Then, AIBN (0.015 mol·L^{-1}) was added. After mixing the solution was transferred into threaded glasses (20 mL). The glasses were placed in a heating block (Liebisch Labortechnik Labtherm Type 5138–6201) on a circular shaker (IKA Labortechnik KS501 digital, 100 rounds per minute). The reactions were performed at 80 °C and stopped after 15, 30, 45, 60, and 90 min by adding a few drops of methanol containing traces of hydroquinone. A sample without AIBN was prepared to serve as reference at time 0.

2.4. Size-Exclusion chromatography

Size-exclusion chromatography (SEC) analyses were performed using two systems. SEC A consists of a Knauer Marathon autosampler, a Waters 515 HPLC pump, a Knauer Smartline refractive index detector 2300 and a set of three chromatographic columns (100, 1000, 100,000 Å SDV, polymer standards service (PSS, Mainz Germany)). THF was used as eluent at a flow rate of 1 mL•min^{-1}. Calibration was established using seven polystyrene standards with molar masses ranging from 162 to 2.57•10^6 g•mol^{-1} from PSS. The samples to be injected were prepared by diluting 0.2 mL of each reaction mixture with 3.8 mL THF and were filtered with a syringe filter (0.45 µm) prior to injection. A sample volume of 100 µL was used. SEC B consists of an Agilent Technologies 1200 SEC system including a variable UV detector and a refractive index detector. THF was used as eluent at a flow rate of 1 mL•min^{-1}. Separation was achieved using three SDV 1000A columns at 40° C and a sample concentration of 10 mg•mL^{-1}. Calculation of the molar mass distribution was diverted from the calibration with polystyrene in the range of 162 g•mol^{-1} to 70,000 g•mol^{-1}. The samples were filtered over a 0.2 µm PTFE filter prior to injection. Data acquisition and evaluation were conducted with WinGPC Unity software provided by PSS for both SEC systems.

2.5. NMR spectroscopy

The variation in monomer concentrations was measured off-line via ^{1}H NMR spectroscopy using a Magritek Spinsolve 80 MHz ULTRA Carbon instrument. Samples of 0.5 mL were taken straight from the reaction mixture and measured at room temperature in the solvent suppression mode “WET SUP” allowing for the use of non-deuterated 1,4-dioxane as solvent. Proton chemical shifts were reported in ppm relative to the residual solvent protons of 1,4-dioxane at 3.53 ppm. For measurement of high-field NMR spectra an “Avance Neo 400 MHz” digital FT-NMR spectrometer with iProbe BBF/H/F and BBO sample head (Bruker BioSpin GmbH & Co. KG, Ettlingen, Germany) was used. The cryomagent has a magnetic flux density of 9.4 T and a proton frequency of 400 MHz. Deuterated dioxane-d_8 was used as solvent. The ^{1}H NMR spectrum of DTHFI in deuterated chloroform-d_1 was recorded using an “Avance III 600 MHz” spectrometer.

2.6. Monte Carlo simulations

The simulation approach was described in detail elsewhere.[17] Input data are the individual concentrations of both monomers throughout the copolymerization, two r values as well as the ratio of the itaconate rate coefficients of propagation and depropagation. The output of the Monte Carlo (MC) simulations consists of the individual concentrations for each monomer as a function of overall monomer conversion. To determine the r values based on the experimental data, the MC simulation was embedded in an optimization environment for a stochastic Metropolis-Hastings optimization environment implemented in Python 3.12.[30] The simulations were executed on a compute server with two AMD Epyc 7H12 processor and Ubuntu 24.04 LTS as the operating system. The MC code and associated files are provided in the Supporting Information.

3. Results and discussion

3.1. Data evaluation with SEC

In order to track the individual conversion of the monomers during copolymerization, samples taken at specific reaction times were analyzed by SEC. The SEC separation method is based on the dependence of the elution time on the hydrodynamic radius of the molecules. Thus, not only the polymers formed during the reaction can be separated from the monomers, but also the two monomers can be distinguished and analyzed individually. The prerequisite is that the hydrodynamic radii of the monomers differ sufficiently. This criterion is met for systems of the three itaconates under consideration with CHA as well as for copolymerizations of DBI or DCHI with butyl acrylate (BA) reported previously.[17] However, clear separation of the itaconates and 2OA or iBoA was not always feasible. As an example, Fig. 2 shows the elution curves for the copolymerization of DBI with iBoA and CHA. As expected, the polymer elutes first and an increase in intensity of the polymer signal with reaction time is observed. At elution times higher than 24 min the peaks assigned to the monomers and at times beyond 25 min to the solvent are visible. The negative peak overlapping the solvent peak may originate from minor amounts of water introduced due to quenching the polymerization with methanol containing traces of hydrochinone. In contrast to the DBI – CHA system with clearly resolved monomer peaks, for DBI – iBoA the peak maxima are distinctly different while the peaks are partially overlapping. For both systems a continuous decrease in peak intensity of both monomers is clearly seen. For mathematical peak separation of the two monomer peaks and calculation of peak areas the program Origin was used. Data analysis was based on fitting Gaussian curves to the elution curves in the range of the monomer elution times. Since the initial concentration of the monomers is known, conversions are accessible from the relative change in peak areas.

Fig. 3 presents the individual monomer conversions derived from SEC elution curves of DBI – iBoA copolymerization mixtures. It is clearly seen that the DBI conversion increases faster than iBoA conversion for initial monomer feed compositions of $f^0_{DBI} = 0.3$ and f^0_{DBI} 0.5, which indicates preferential itaconate incorporation into the copolymer.

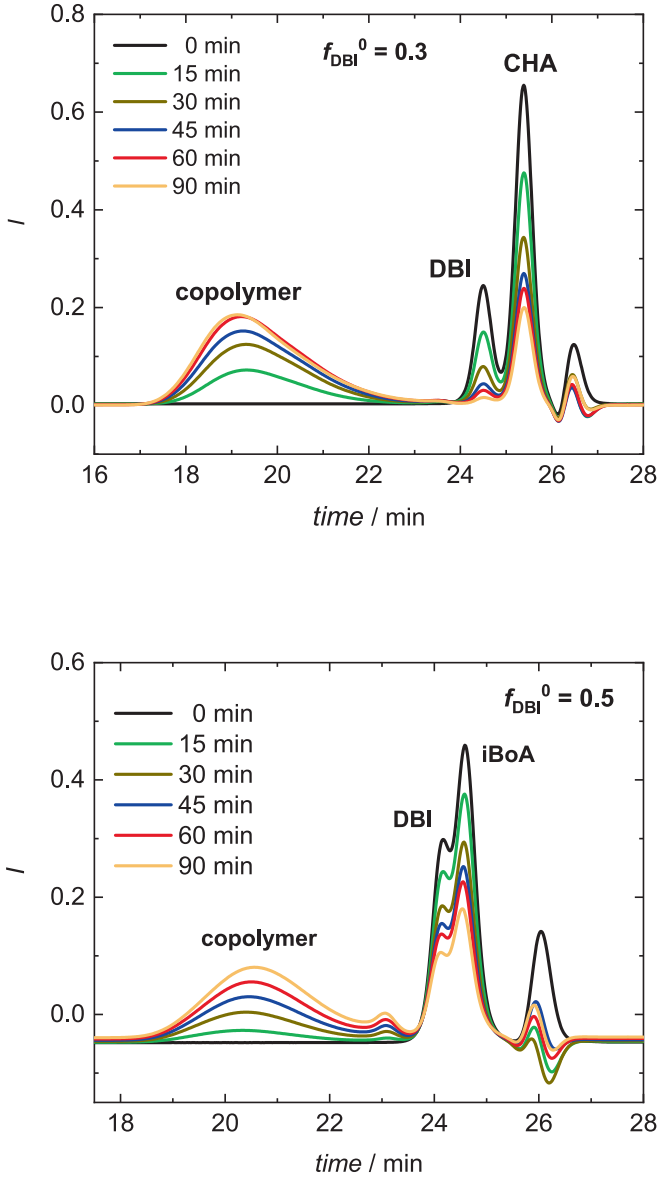

Fig. 2. SEC elution curves for copolymerizations of DBI with CHA (top) and iBoA (bottom) at 80 °C in 50 vol% dioxane. Initial monomer feed compositions are 0.5 and 0.3 for copolymerizations with iBoA and CHA, respectively.

The opposite is observed with $f_{DBI}^0 = 0.7$ in Fig. 3, where the conversion of iBoA is higher than for DBI at all times. It is suggested that the lowering of DBI incorporation at high f_{DBI}^0 is caused by depropagation of itaconate monomer units, which becomes all the more important with a higher itaconate content. Generally, the presence of non-depropagating acrylate moieties limits unzipping of itaconate units at the macroradical chain end. With a lowering of the BA content the probability for removal of itaconate units is enhanced. The observation is in excellent agreement with studies into the copolymerization of styrene and methacrylates, with the latter undergoing depropagation.[31] Conversion – time data for the other copolymerization systems provided in Fig. S4 to S10 of the Supporting Information show the same result.

Moreover, the temporal development of itaconate consumption at different f_{DBI}^0 shows that substantially higher conversion of both monomers is reached with a lower initial itaconate content at the selected reaction time of 90 min. As an example, DBI – iBoA copolymerization with $f_{DBI}^0 = 0.3$ results in DBI conversion of 27 % at 15 min and 94 % at 90 min. The corresponding conversions for $f_{DBI}^0 = 0.7$ are 15 % and 32 %, respectively. This observation illustrates a low overall reaction rate with

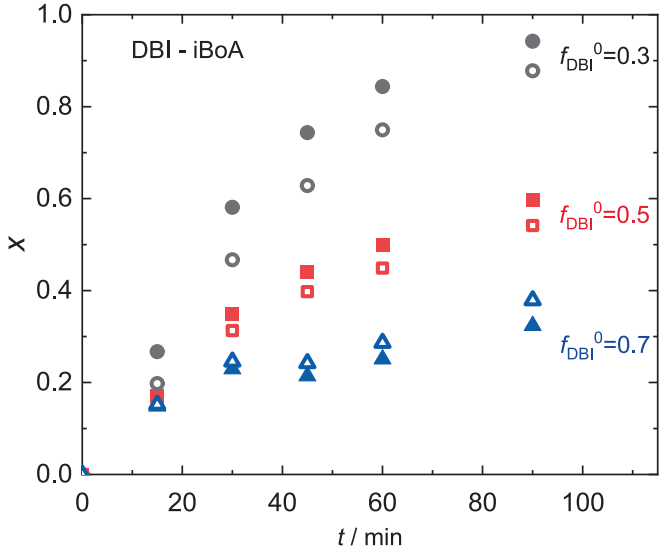

Fig. 3. Conversion-time curves for copolymerizations of DBI and iBoA at 80 °C with f_{DBI}^0 as indicated. Open markers refer to iBoA, filled markers to DBI.

high itaconate content, which is again suggested to be due to depropagation and low itaconate k_p.

In addition to depicting the monomer concentration as a function of time, the monomer concentrations are given relative to each other in Fig. 4. It is clearly seen that the concentration changes are very similar for all itaconate – iBoA systems over the course of the reaction, which indicates minor influence of the itaconate ester groups under investigation on copolymer composition in copolymerizations with iBoA. The arrow indicates that the reaction proceeds towards low concentration.

Tracking the conversion of the copolymerization by means of SEC provides molar mass distributions (MMDs) of the resulting copolymers from the same analyses. Fig. 5 gives MMDs for the itaconate – iBoA copolymers. For clarity of presentation the distributions for copolymerizations with DBI are not shown. For DCHI, it is clear that a higher fraction of itaconate in the monomer feed results in lower molar masses, which is suggested to be due to the significantly lower itaconate propagation rate compared to the acrylate. In addition to the main peak,

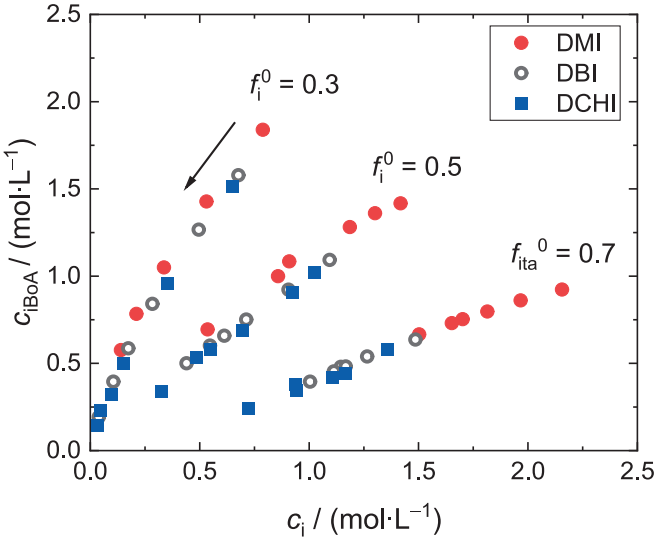

Fig. 4. Variation of iBoA concentration as a function of itaconate concentration derived from SEC measurements for copolymerizations of DMI, DBI, and DCHI with iBoA at 80 °C and the indicated initial itaconate feed ratios f_i^0. Polymerization proceeds towards low concentrations, as illustrated by the arrow.

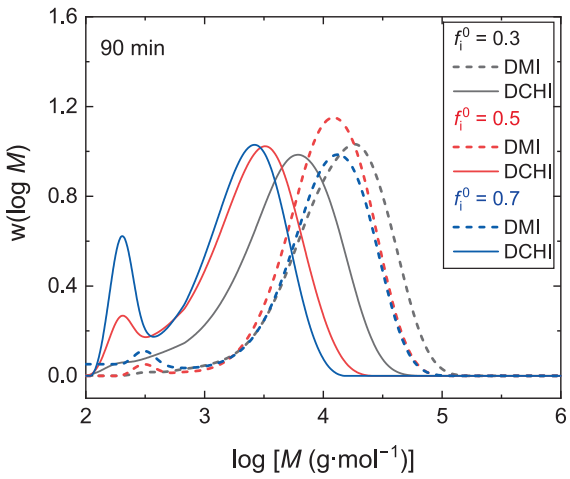

Fig. 5. Molar mass distributions of the copolymers from copolymerizations of DMI and DCHI with iBoA at the indicated itaconate feed ratios. Molar masses refer to SEC calibration with polystyrene standards.

a second peak between 100 and 1000 g•mol^{-1} is noticeable, which is most pronounced for $f^0_{DCHI} = 0.7$, while the peak is only of minor intensity for $f^0_{DCHI} = 0.3$. The peak is suggested to originate from intramolecular chain transfer to polymer, so-called backbiting. While itaconates were supposed to undergo some backbiting,[32] acrylates are well-known to undergo significant backbiting converting most of the secondary propagating radicals to so-called midchain radicals.[33,34] On the contrary, for copolymerizations with DMI significantly higher molar masses are observed, which is suggested to be due to an enhancement of the itaconate propagation rate coefficient with decreasing ester size[9,11,12] In addition, a lowering of the diffusion-controlled termination rate coefficient is observed with increasing ester group.[9].

Moreover, the position of the MMD for f^0_{DMI} of 0.5 and 0.7 is very similar. Slightly higher molar masses are observed for the lowest f^0_{DMI} of 0.3. Further, the copolymer MMD obtained from polymerization with the lowest DMI content in the monomer feed, f^0_{DMI} of 0.3, is monomodal, lacking the low molar mass peak. The MMDs originating from polymerization with f^0_{DMI} of 0.5 and 0.7 feature a low molar mass peak which is substantially smaller than that of the DCHI copolymers. The differences observed in comparison to the DCHI – BA copolymerizations indicate that investigations into the detailed polymerization mechanism and kinetics are mandatory for simulation of the copolymerizations and prediction of the polymer microstructure.

Fig. 2 indicates that the SEC elution peaks of the itaconate and the acrylate monomer are not always as well-separated as for DBI – BA[17] or DBI – CHA copolymerizations and peak deconvolution is required prior to determination of individual monomer concentrations. In order to validate the SEC-based results, in addition, ^{1}H NMR spectroscopy was applied.

3.2. Data evaluation based on ^{1}H NMR spectra

Previously, in-line ^{1}H NMR spectroscopy (400 or 600 MHz) was applied to monitor DBI – BA polymerizations. The reactions were carried out either directly inside the spectrometer or off-line using samples that were quenched at different reaction times.[16,17] Detailed information on the peak assignment was reported.

Rather than recording high-field NMR spectra, here spectra were recorded mostly with an 80 MHz benchtop NMR instrument. The use of a benchtop NMR spectrometer is advantageous since the spectra are recorded directly in the laboratory without significant time delay. Moreover, deuterated solvents are not required. However, the low resolution of the 80 MHz benchtop NMR and the large number of signals from the vinyl protons of two monomers render signal separation difficult. As an example, Fig. S11 of the supporting information provides the spectra of iBoA and DBI. An assignment of the vinyl protons in the spectrum of the mixture of DBI and iBoA is shown in Fig. 6 by color coding. The signals that were integrated to calculate monomer conversion are also marked in red (acrylate) and purple (itaconate). The calculation of monomer concentrations and temporal changes of the signals assigned to monomer and copolymer are contained in the Supporting Information.

As above-mentioned, separation of the monomer peaks is limited by the resolution of the low field benchtop NMR spectrometer. In order to validate the conversion data obtained, they are compared to data from other analytical methods for selected systems. For the DMI-2OA system, a comparison with SEC A is carried out. As DMI contains the short methyl ester groups, the separation capability of the SEC columns is sufficient to resolve the peaks assigned to the monomers. Results for the DBI-2OA system are compared to data derived with SEC B, which is equipped with three SDV 1000A columns with higher resolution at low molar masses intended for the separation of oligomers. Further, results for the DBI-iBoA system are compared to data derived from SEC A and from ^{1}H NMR spectra recorded with a 400 MHz spectrometer. The concentrations obtained from the various analytical methods depicted in Fig. S13 of the Supporting Information show very good agreement. Thus, the resolution of the 80 MHz NMR instrument is well-suited for the determination of the individual monomer concentrations throughout the copolymerizations.

While in Fig. 4 relative concentrations for a given acrylate with different itaconates were addressed, Fig. 7 shows data for DBI copolymerized with all acrylates under consideration. For $f^0_{DBI} = 0.5$ and $f^0_{DBI} = 0.7$ the concentration profiles at a given initial DBI feed are very similar, regardless of the size and structure of the acrylate ester group. Only for the lowest f^0_{DBI} of 0.3 some deviations are seen during the course of the polymerization at residual concentrations below 0.5 mol•L^{-1} for DBI and 1 mol•L^{-1} for BA and CHA. On the contrary, for copolymerizations with iBoA and 2OA no distinct deviations are seen. The finding is suggested to be due to backbiting of acrylate units in the macroradicals and subsequent reactions of the MCRs formed. Previously, it was discussed that the addition of an iBoA monomer molecule compared to a BA molecule proceeds slower due to the sterically demanding *i*-bornyl group.[35] As a consequence the branching level (*BL*) depends on the type of acrylate ester group. Recently, for poly(iBoA) a minor *BL* was found, whereas for poly(CHA) and poly(BA) substantially higher *BL* were observed,[36] also indicating that the ester group may have an influence on backbiting and the associated follow-up reactions.

3.3. Determination of reactivity ratios

Reactivity ratios were determined for all systems employing Monte Carlo simulations, which were described in detail elsewhere.[17] Rather than accounting for all elemental reactions of the full kinetic scheme, the simulations are based on the probability of adding one of the two monomers to the macroradical chain end. In the case of a propagating radical with two itaconate monomers at the end of the chain, the probability of depropagation was also considered, this requires the ratio of the rate coefficients k_p and k_{dep}. The temperature dependence of both rate coefficients was already reported for DMI, DBI, and DCHI.[11] The Arrhenius parameters are listed in Table S3 and Table S4 of the Supporting Information.

Since the concentration diagrams for most systems under investigation are very similar and because a strong family-type behavior was observed for propagation within the families of acrylates, methacrylates, and itaconates, the data set containing experimental data from all monomer pairs was analyzed. MC simulations were performed considering the combined data set of 186 concentration tuples derived from SEC and NMR analyses and parameter estimation using the Metropolis Hastings algorithm. The final optimization run was performed in the

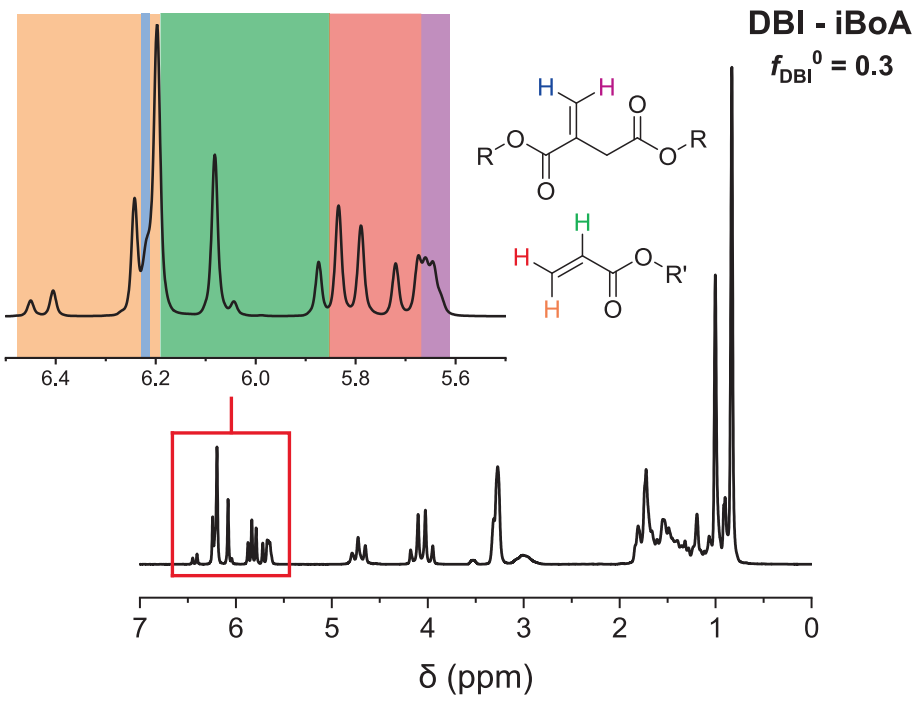

Fig. 6. ^{1}H NMR spectrum (80 MHz) of a DBI-iBoA mixture with an enlarged view of the olefinic region and assignment of the olefinic proton peaks.

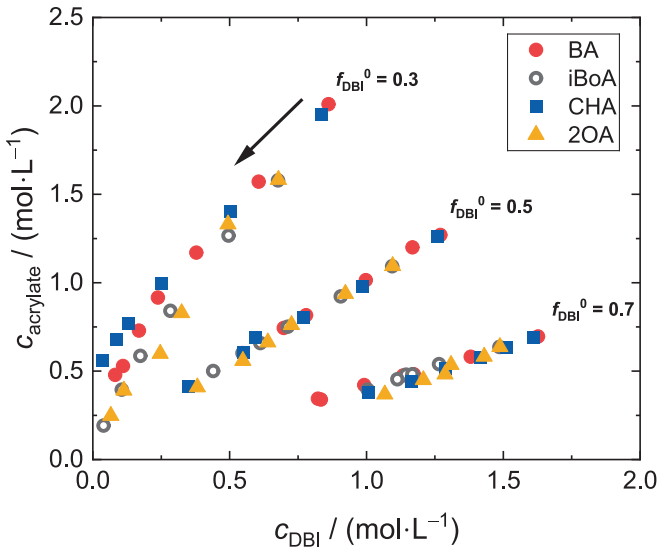

Fig. 7. Variation of acrylate concentration with DBI concentration during copolymerization of various acrylates with DBI at 80 °C. Polymerization proceeds towards low concentrations, as illustrated by the arrow.

range $0.5 < r_i < 2.5$ and $0.1 < r_a < 1.5$. A total of more than 40,000 optimization steps were performed and terminated when no improved result was obtained after 5000 steps. The combined data set is very well represented by $r_i = 1.50$ and $r_a = 0.54$, which is indicated by the lines in Fig. 8. Only the data obtained for the system DBI – CHA with $f_{DBI}^0 = 0.3$ (open grey circles in Fig. 8B) were excluded, because Fig. 7 indicates the largest deviation from all other concentration curves for this data. The *r* values determined also provide a decent representation of the data excluded from the combined data set.

In the Monte Carlo simulation, the acrylate concentration is calculated as a function of the itaconate concentration. The output is based on the experimentally determined itaconate concentrations. This results in deviations between the experiment and simulation for the acrylate concentrations, which are shown as a parity plot in Fig. 9. The itaconate / acrylate systems shown in black were used to determine the *r* values. Substantial differences between the various systems are not seen. Further, a similar evaluation of the data derived with different analytical methods (SEC vs. 80 MHz/400 MHz NMR) is presented in Fig. S14, indicating similar levels of precision in all cases. The common *r* values determined for the ten copolymerization systems listed in Table S1 were transferred to the copolymerization test systems of DTHFI/BA as well as DMI/NIPAM and DBI/NIPAM. Again, good agreement of the simulated and experimentally derived data is found.

The concentration diagrams in Fig. 8 indicate that full itaconate conversion is not achieved for high initial itaconate feed ratios of $f_i^0 \geq 0.5$ in any of the systems, which is assigned to significant contributions from depropagation at 80 °C and high fractions of itaconate. However, it should be noted that the residual itaconate concentrations are substantially lower than the equilibrium monomer concentrations of 1.10, 1.34, and 1.20 mol•L^{-1} calculated from the ratio k_{dep}/k_p for homopolymerizations of DMI, DBI, and DCHI, respectively. As an example, for copolymerizations with $f_i^0 = 0.7$ residual DBI concentrations range from 0.4 to 0.5 mol•L^{-1}, which are 37 % lower than the equilibrium monomer concentration of 1.34 mol•L^{-1} for DBI homopolymerization at the same temperature. Thus, due to the presence of the acrylate comonomer monomer conversion is less limited as for itaconate homopolymerizations.

In addition, information on the impact of the actual itaconate monomer concentration on the probability of depropagation to occur is accessible from the Monte Carlo simulations. Propagation of iBoA, DBI, or depropagation of DBI can occur on a polymer chain with a sequence of at least two BDI monomers at the chain end. During the Monte Carlo simulation, these reaction steps are counted and the ratio of depropagation to propagation of DBI can be calculated, which is shown in Fig. 10. Since the comonomer iBoA influences the sequence length of DBI at the chain end, this ratio also depends on the comonomer composition. Due to depropagation, complete conversion of DBI will not be achieved for $f_{DBI}^0 = 0.7$ and $f_{DBI}^0 = 0.5$.

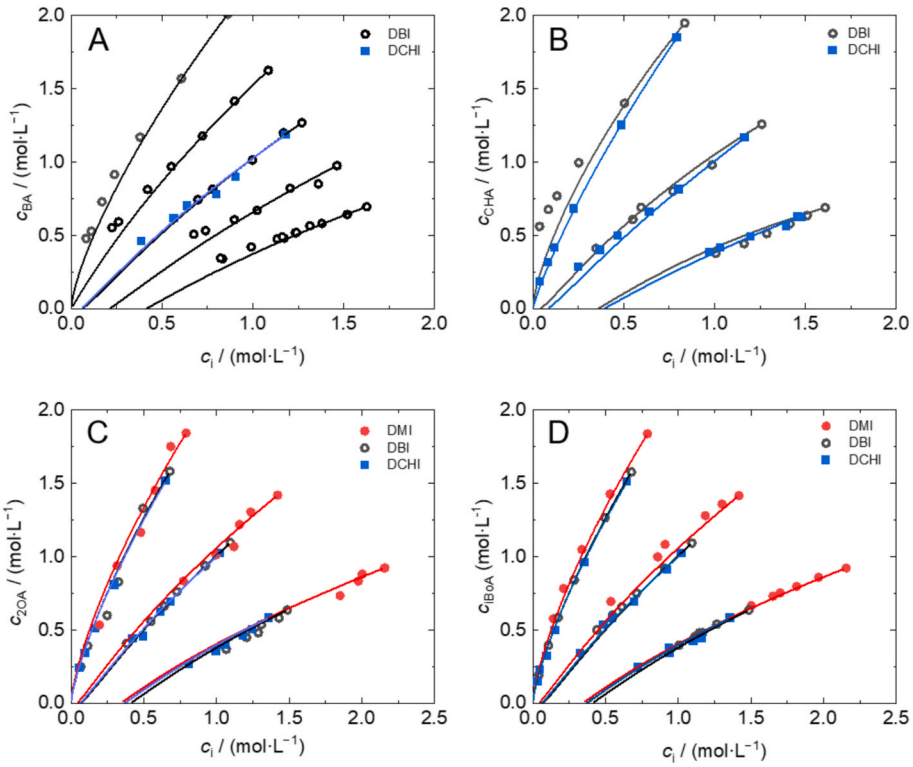

Fig. 8. Variation of butyl acrylate (A), cyclohexyl acrylate (B), 2-octyl acrylate (C), and i-bornyl acrylate (D) concentrations with itaconate concentrations determined for copolymerizations at 80 °C. The symbols refer to experimental data, and the lines indicate the results from the MC simulations using $r_i = 1.50$ and $r_a = 0.54$.

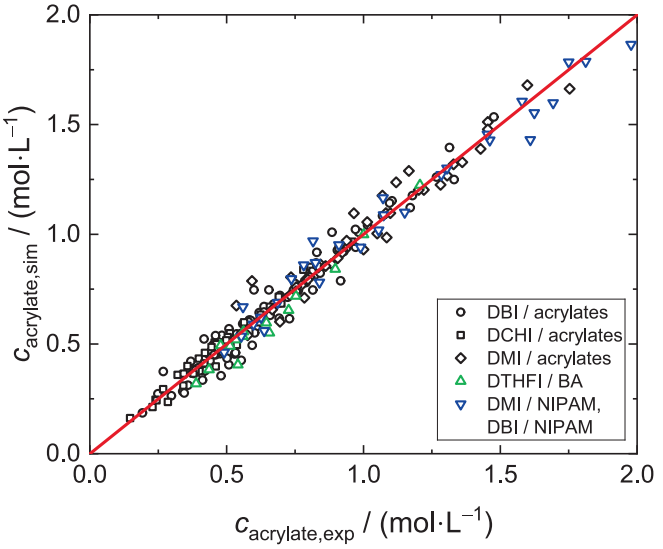

Fig. 9. Comparison of acrylate concentration derived from simulation and experiment for any moment in time.

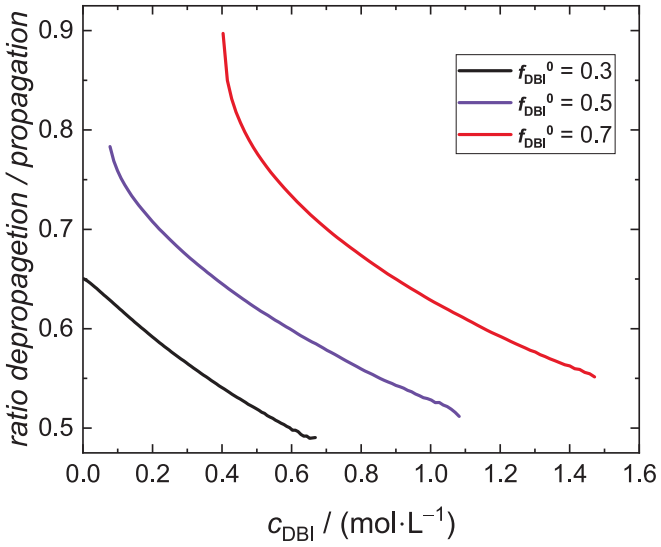

Fig. 10. Simulated ratio of DBI depropagation to DBI propagation steps for copolymerizations of DBI with iBoA at 80 °C and the indicated initial DBI monomer feed compositions.

3.4. *Transferability of reactivity ratios to other copolymerizations systems*

Since all data is well represented by a single set of reactivity ratios it appeared attractive to test whether this data is also applicable to other copolymerization systems involving diesters of itaconic acid. The first example comprises copolymerizations of DTHFI and BA, where both monomers are not expected to undergo specific interactions. The concentration diagram obtained for copolymerizations at 80 °C with f_i^0 of 0.3, 0.5 and 0.7 is presented in Fig. 11. Since the rate coefficients for k_p and k_{dep} are not yet known for DTHFI, firstly the average of k_{dep}/k_p of DMI, DBI, and DCHI at 80 °C was calculated. The resulting value of 1.2 was used to simulate the variation of BA and DTHFI concentration during the copolymerization. The black line in Fig. 11 refers to this data. An excellent agreement with the experimental data obtained for $f_i^0 = 0.3$ is seen. This demonstrates that the generalized r values can also be applied to describe the copolymerization of DTHFI with BA. It should be noted that depropagation has the lowest influence on the relative incorporation of the monomers in this composition range. For higher DTHFI contents in the monomer feed a slight deviation is seen. Still, the

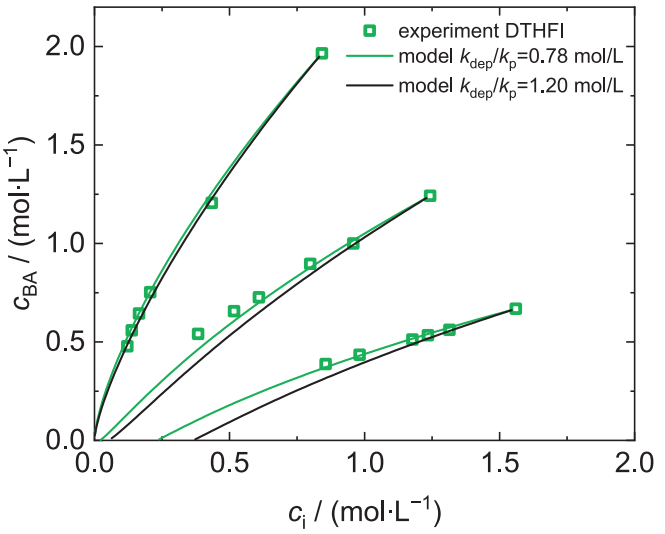

Fig. 11. Variation of butyl acrylate concentrations with DTHFI concentration determined for copolymerizations at 80 °C. The symbols refer to experimental data, and the lines indicate the results from the MC simulations using $r_i = 1.50$ and $r_a = 0.54$ and the indicated ratios of k_{dep}/k_p.

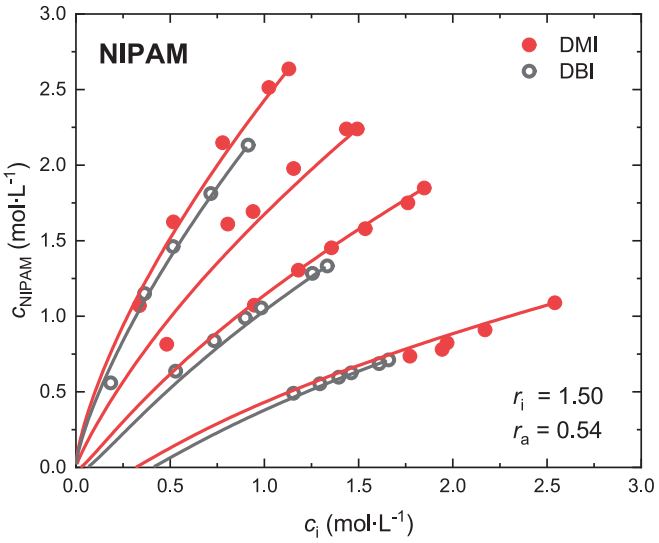

Fig. 12. Variation of NIPAM concentrations with DMI and DBI concentration determined for copolymerizations at 80 °C. The symbols refer to experimental data, and the lines indicate the results from the MC simulations using $r_i = 1.50$ and $r_a = 0.54$ and the k_{dep}/k_p values taken from literature.

agreement is remarkable.

Secondly, MC simulations with the reactivity ratios $r_i = 1.50$ and $r_a = 0.54$ being fixed were carried out in order to estimate the ratio of k_{dep}/k_p by systematic variation in the range from 0.1 to 2.0 mol•L^{-1} with increments of 0.01 mol•L^{-1}. The optimization yields a k_{dep}/k_p of 0.78 mol•L^{-1}, which is slightly lower than the corresponding values of 1.10, 1.20, and 1.34 mol•L^{-1} for DMI, DCHI, and DBI, respectively, and higher than the value of 0.44 mol•L^{-1} for di(4-*tert*-butyl cyclohexyl) itaconate with two sterically demanding ester groups.[11] The green line in Fig. 11 represents the corresponding concentration data, which are in excellent agreement with the experimental data. The transfer of the data obtained for the DMI, DCHI, and DBI systems to DTHFI is in line with a family-type behavior for non-functional esters observed for acrylates and methacrylates.[37].

The second example addresses DMI and DBI copolymerizations with N-isopropyl acrylamide (NIPAM). NIPAM was selected, because it is a derivative of acrylic acid and a similar copolymerization behavior with itaconate monomers was anticipated. Moreover, poly(NIPAM) and several copolymers of NIPAM are well-known as temperature switchable materials,[38] making NIPAM an attractive comonomer with respect to temperature responsive materials. The concentration data for both NIPAM systems given in Fig. 12 looks very similar to the other systems discussed above. Therefore, the variation of NIPAM concentration c_{NIPAM} with itaconate concentration was calculated for both comonomer systems with reactivity ratios of $r_i = 1.50$ and $r_a = 0.54$. The above-mentioned k_{dep}/k_p values of 1.10 and 1.34 mol•L^{-1} for DMI and DBI, respectively, were used. The agreement of the experimental and simulated concentration data for the NIPAM systems is excellent.

Both transferability examples indicate that the reactivity ratios for itaconates with acrylate-type monomers are dominated by the general monomer structure and are almost independent of the ester groups selected. The finding is in good agreement with findings for copolymerizations of acrylates with methacrylates with either methyl or dodecyl ester groups.[37] Regardless whether both ester groups were identical or different, all systems were described by a single set of reactivity ratios. In contrast, the copolymerization propagation rate coefficients, k_p^{copo}, were strongly different for the comonomer systems.[37] For the itaconate – acrylate systems under investigation it remains to be tested to which extent k_p^{copo} is affected by the ester groups, because k_p of both monomer families are much more different than in the case of acrylates and metharylates. Further, the study needs to be extended to monomers carrying functional groups. In particular monomers with OH groups may lead to deviations, since it is well known that the propagation reaction is strongly affected by H bonding with the carbonyl group.[39–41].

4. Conclusions

Itaconate – acrylate copolymerizations were considered to overcome challenges associated with itaconate radical homopolymerizations, such as slow propagation rate and limited monomer conversion due to depropagation. Ten comonomer systems consisting of itaconates and acrylates with several ester groups were studied aiming for general insights into the impact of the ester group on copolymer composition. *r* values were determined from copolymerizations up to high conversions with individual monomer conversions derived from ^{1}H NMR spectra and SEC elution curves. Excellent agreement of the data derived from the different analytical methods is observed.

Determination of the reactivity ratios was achieved via Monte Carlo simulations accounting for depropagation of itaconate monomers. The large set of composition data from 186 individual analyses for copolymerizations of DMI, DBI, and DCHI with iBoA, CHA, 2OA, and BA is described by a single set of *r* values of 1.50 and 0.54 for itaconates and acrylates, respectively. Based on this remarkable finding it was tested whether this pair of *r* values derived from 10 comonomer mixtures can also be applied to additional comonomer pairs. Two test cases were studied: the copolymerization of DTHFI with BA as well as DMI and DBI with NIPAM as acrylic component. Very good description of both monomer concentrations throughout the copolymerization was observed for both test cases. The findings may be explained with a strong family-type behavior: because k_p values of itaconates and acrylates differ by around three to four orders of magnitude, small variations in k_p within the group of itaconates and within the group of acrylic monomers are not reflected by the *r* values. Although the *r* values are not significantly altered by the ester group selected, the copolymerization propagation rate coefficient may be affected by the ester groups. In future studies, these kinetic coefficients need to be determined in order to simulate the copolymerization process.

The monomers used in this study do not contain functional groups undergoing specific interactions, for example such as substantial hydrogen bonding. As previously shown, in cases with strong H bonds between the OH and the carbonyl groups of the monomer units, a strong

impact on the propagation rate coefficients as well as on the copolymer composition are suggested to occur. In these cases, deviations from the general trend observed here are likely. Thus, copolymerizations of monomers with functional ester groups are the topic of future studies.

CRediT authorship contribution statement

Lennart Arendes: Writing – review & editing, Writing – original draft, Visualization, Validation, Investigation, Formal analysis, Data curation. **Marco Drache:** Writing – review & editing, Validation, Software, Formal analysis, Data curation. **Celine Bösche:** Investigation, Data curation. **Tobias Robert:** Writing – review & editing, Supervision, Project administration, Methodology, Investigation, Funding acquisition, Conceptualization. **Sabine Beuermann:** Writing – review & editing, Writing – original draft, Visualization, Supervision, Methodology, Investigation, Funding acquisition, Conceptualization.

Declaration of competing interest

The authors declare the following financial interests/personal relationships which may be considered as potential competing interests: Robert, Tobias reports financial support was provided by Federal Ministry of Education and Research Bonn Office. If there are other authors, they declare that they have no known competing financial interests or personal relationships that could have appeared to influence the work reported in this paper.

Acknowledgements

Funding from German Ministry of Education and Research (BMBF) within the project BioSwitchit (FKZ: 031B1419A) is gratefully acknowledged. The authors thank Xueqi Guo for the help with the SEC measurements and Alexander Omelan for TGC/MS measurements.

Appendix A. Supplementary data

Supplementary data to this article can be found online at https://doi.org/10.1016/j.eurpolymj.2025.114305.

Data availability

All data are included in the Supporting Information. There is no more data than contained in the Supporting Information.

References

[1] A. Kuenz, S. Krull, Biotechnological production of itaconic acid – things you have to know, Appl. Microbiol. Biotechnol. 102 (2018) 3901–3914, https://doi.org/10.1007/s00253-018-8895-7.
[2] S. Krull, M. Lünsmann, U. Prüße, A. Kuenz, Ustilago Rabenhorstiana - an Alternative Natural Itaconic Acid producer, Fermentation 6 (2020) 4, https://doi.org/10.3390/fermentation6010004.
[3] T. Robert, S. Friebel, Itaconic acid a versatile building block for renewable polyesters with enhanced functionality, Green Chem. 18 (2016) 2922–2934, https://doi.org/10.1039/c6gc00605a.
[4] S. Pérocheau Arnaud, N.M. Malitowski, K. Meza Casamayor, T. Robert, Itaconic acid-based reactive diluents for renewable and acrylate-free UV-curing additive manufacturing materials, ACS Sustainable, Chem. Eng. 9 (2021) 17142–17151, https://doi.org/10.1021/acssuschemeng.1c06713.
[5] S. Pérocheau Arnaud, E. Andreou, L.V.G. Pereira Köster, T. Robert, Selective synthesis of monoesters of itaconic acid with broad substrate scope: biobased alternatives to acrylic acid? ACS Sustain, Chem. Eng. 8 (2020) 1583–1590, https://doi.org/10.1021/acssuschemeng.9b06330.
[6] P. Li, S. Ma, J. Dai, X. Liu, Y. Jiang, S. Wang, J. Wei, J. Chen, J. Zhu, Itaconic acid as a green alternative to acrylic acid for producing a soybean oil-based thermoset: synthesis and properties, ACS Sustain. Chem. Eng. 5 (2017) 1228–1236, https://doi.org/10.1021/acssuschemeng.6b02654.
[7] Y. Zhu, Z. Hua, Y. Song, W. Wu, X. Zhou, J. Zhou, J. Shi, Highly chemoselective esterification for the synthesis of monobutyl itaconate catalyzed by hierarchical porous zeolites, J. Catal. 299 (299) (2013) 20–29, https://doi.org/10.1016/j.jcat.2012.11.034.
[8] I. Sollka, K. Lienkamp, Progress in the Free and Controlled Radical Homo- and Co-Polymerization of Itaconic Acid Derivatives: Toward Functional Polymers with Controlled Molar Mass distribution and Architecture, Macromol. Rapid Commun. 42 (2021) 2000546, https://doi.org/10.1002/marc.202000546.
[9] T. Sato, S. Inui, H. Tanaka, T. Ota, Kinetics and ESR Studies on the Radical Polymerization of Di-n-butyl Itaconate in Benzene, J. Polym. Sci., Polym. Chem. Ed. 25 (1987) 637–652, https://doi.org/10.1002/pola.1987.080250216.
[10] H. Kattner, M. Buback, Propagation and Chain-Length Dependent termination Rate Coefficients Deduced from a Single SP-PLP-EPR experiment, Macromolecules 49 (2016) 3716–3722, https://doi.org/10.1021/acs.macromol.6b00483.
[11] Z. Szablan, M.H. Stenzel, T.P. Davis, L. Barner, C. Barner-Kowollik, Depropagation Kinetics of Sterically Demanding Monomers: a Pulsed Laser size Exclusion Chromatography Study, Macromolecules 38 (2005) 5944–5954, https://doi.org/10.1021/ma050444l.
[12] E. Meyer, T. Weege, P. Vana, Free-Radical Propagation Rate Coefficeints of Diethyl Itaconate and Di-n-Propyl Itaconate Obtained via PLP-SEC, Polymers 15 (2023) 1345, https://doi.org/10.3390/polym15061345.
[13] R.A. Hutchinson, D.A. Paquet, S. Beuermann, J.H. McMinn, Investigation of methacrylate free-radical depropagation kinetics by pulsed-laser polymerization, Ind. Eng. Chem. Res. 37 (1998) 3567–3574, https://doi.org/10.1021/ie980167p.
[14] S. Beuermann M. Buback T.P. Davis R.G. Gilbert R.A. Hutchinson Critically evaluated rate coefficients for free-radical polymerization, 3. Propagation rate coefficients for alkyl methacrylates Macromol. Chem. Phys. 12 %3C1355::AID-MACP1355%3E3.0.CO;2-Q 201 (2000), 1355 1364 10.1002/1521-3935 (20000801)201.
[15] N. Ballard, J.M. Asua, Radical polymerization of acrylic monomers: an overview, Prog. Polym. Sci. 79 (2018) 40–60, https://doi.org/10.1016/j.progpolymsci.2017.11.002.
[16] T. Pirmin, C.A. Sanders, M. Ocepek, M.F. Cunningham, B. Likozar, R. A. Hutchinson, Free radical copolymerization kinetics of bio-based dibutyl itaconate and n-butyl acrylate, Chem. Eng. J. 2499 (2024) 156127, https://doi.org/10.1016/j.cej.2024.156127.
[17] M. Drache, B.A. Tameno Kouanwo, J. C. Namyslo, S. Pérocheau Arnaud, T. Robert, S. Beuermann, Reactivity Ratios of Biobased Dialkyl Itaconate Radical Polymerizations Derived from In-Line NMR Spectroscopy and Size-Exclusion Chromatography, ACS Polymers Au 4 (2024) 540-549, Doi: 10.1021/acspolymersau.4c00071.
[18] A. Badia, J. Movellan, M.J. Barandiaran, J.R. Leiza, High Biobased Content Latexes for Development of Sustainable pressure Sensitive Adhesives, Ind. Eng. Chem. Res. 57 (2018) 14509–14516, https://doi.org/10.1021/acs.iecr.8b03354.
[19] R.G. Gilbert, Emulsion Polymerization: a Mechanistic Approach, Academic Press Limited, London, 1995.
[20] S.C. Thicket, R.G. Gilbert, Emulsion polymerization: State of the art in kinetics and mechanisms, Polymer 48 (2007) 6965–6991, https://doi.org/10.1016/j.polymer.2007.09.031.
[21] L. Arendes, Emulsionspolymerisationen biobasierter Methacrylate und Itaconate, Master Thesis, Clausthal University of Technology, 2024.
[22] S.C. Fischer von Mollard, N. Ueberschaar, M. Schreiber, F. Kamphuis, S. Zechel, M. D. Hager, Synthesis of Poly(itaconate)s with High Monomer Conversion applying Emulsion Polymerization, J. Polym. Sci. 63 (2025) 1284–1296, https://doi.org/10.1002/pol.20240414.
[23] J. Gupta, R. Tomovska, M. Aguirre, Overcoming challenges of Incorporation of Biobased Dibutyl Itaconate in (Meth)acrylic Waterborne Polymers, Biomacromolecules 25 (2024) 5310–5320, https://doi.org/10.1021/acs.biomac.4c00739.
[24] A.A.A. Autzen, S. Beuermann, M. Drache, C.M. Fellows, S. Harrisson, A.M. van Herk, R.A. Hutchinson, A. Kajiwara, D.J. Keddie, B. Klumperman, G.T. Russell, IUPAC Recommended Experimental Methods and Data Evaluation Procedures for the Determination of Radical Copolymerization Reactivity Ratios from Composition Data, Polym. Chem. 15 (2024) 1851–1861, https://doi.org/10.1039/D4PY00270A.
[25] E. Möller, U. Schreiber, S. Beuermann, In Line Spectroscopic Investigation of FluorinatedCopolymer Synthesis in Supercritical Carbon Dioxide, Macromol. Symp. 289 (2010) 52–63, https://doi.org/10.1002/masy.200900007.
[26] I. Zapata-González, E. Saldívar-Guerra, R.A. Hutchinson, 80 years of the Mayo Lewis equation. a comprehensive review on the numerical estimation techniques for the reactivity ratios in typical and emerging copolymerizations, Prog. Polym. Sci. 163 (2025) 101956, https://doi.org/10.1016/j.progpolymsci.2025.101956.
[27] D.J. Lundberg, L.J. Kilgallon, J.C. Cooper, F. Starvaggi, Y. Xia, J.A. Johnson, Accurate Determination of Reactivity Ratios for Copolymerization Reactions with Reversible propagation Mechanisms, Macromolecules 57 (2024) 6722–6740, https://doi.org/10.1021/acs.macromol.4c00835.
[28] W. Jakubowski, A. Juhari, A. Best, K. Koynov, T. Pakula, K. Matyjaszewski, comparison of thermomechanical properties of statistical, gradient and block copolymers of isobornyl acrylate and n-butyl acrylate with various acrylate homopolymers, Polymer 49 (2008) 1567–1578, https://doi.org/10.1016/j.polymer.2008.01.047.
[29] S. Beuermann, S. Harrisson, R.A. Hutchinson, T. Junkers, G.T. Russell, Update and critical Reanalysis of IUPAC Benchmark Propagation Rate Coefficient Data, Polym. Chem. 13 (2022) 1891–1900, https://doi.org/10.1039/D2PY00147K.
[30] A. Feuerpfeil, M. Drache, L.-A. Jantke, T. Melchin, J. Rodríguez-Fernández, S. Beuermann, Modeling complex semi-batch vinyl acetate polymerization processes, Ind. Eng. Chem. Res. 60 (2021) 18256–18267, https://doi.org/10.1021/acs.iecr.1c03114.
[31] S. Beuermann, M. Buback, M. Gadermann, M. Jürgens, F. Günzler, Continuous Styrene – Methyl Methacrylate – Glycidyl Methacrylate Terpolymerizations in

Homogenous Mixtures with Supercritical Carbon Dioxide, Macromol. Symp. 206 (2004) 229–239, https://doi.org/10.1002/masy.200450218.
[32] T. Hirano, R. Takeyoshi, M. Seno, T. Sato, Chain-transfer Reaction in the Radical Polymerization of Di-n-butyl Itaconate at High Temperatures, J. Polym, Sci. Polym. Chem. 40 (2002) 2415–2426, https://doi.org/10.1002/pola.10316.
[33] J. Barth, M. Buback, P. Hesse, T. Sergeeva, EPR analysis of n-butyl acrylate radical polymerization, Macromol. Rapid Commun. 30 (2009) 1969–1974, https://doi.org/10.1002/marc.200900531.
[34] E. Sato, T. Emoto, P.B. Zetterlund, B. Yamada, Influence of mid-chain radicals on acrylate free radical polymerization: effect of ester alkyl group, Macromol. Chem. Phys. 205 (2004) 1829–1839, https://doi.org/10.1002/macp.200400140.
[35] N. Heidarzadeh, E.C. Bygott, R.A. Hutchinson, Exploiting Addition-Fragmentation Reactions to produce Low Dispersity Poly(isobornyl acrylate) and Blocky Copolymers by Semibatch Radical Polymerization, Macromol. Rapid Commun. 41 (2020) 2000288, https://doi.org/10.1002/marc.202000288.
[36] J. Mätzig, Investigation of the high-temperature polymerization of acrylates on the basis of experimental data and kinetic Monte Carlo simulations, PhD Thesis, Clausthal-Zellerfeld (2023).
[37] M. Buback, E. Müller, Propagation Kinetics of Binary Acrylate – Methacrylate Free-Radical Bulk Copolymerizations, Macromol. Chem. Phys. 208 (2007) 581–593, https://doi.org/10.1002/macp.200600547.
[38] H.G. Schild, Poly(N-isopropylacrylamide): experiment, theory and application, Prog. Polym. Sci. 17 (1992) 163–249, https://doi.org/10.1016/0079-6700(92)90023-R.
[39] S. Beuermann, D. Nelke, The influence of hydrogen bonding on the propagation rate coefficient in free-radical polymerizations of hydroxypropyl methacrylate, Macromol. Chem. Phys. 204 (2003) 460–470, https://doi.org/10.1002/macp.200390013.
[40] S. Beuermann, Solvent influence on propagation kinetics in radical polymerizations studied by pulsed laser initiated polymerization, Macromol. Rapid Commun. 30 (2009) 1066–1088, https://doi.org/10.1002/marc.200900131.
[41] J.E.S. Schier, R.A. Hutchinson, The influence of hydrogen bonding on radical chain-growth parameters for butyl methacrylate/2-hydroxyethyl acrylate solution copolymerization, Polym. Chem. 27 (2016) 4567–4574, https://doi.org/10.1039/C6PY00834H.